

ANL/CMT/CP--88661
CONF-960804--41

STAINLESS STEEL-ZIRCONIUM ALLOY WASTE FORMS*

by

S. M. McDeavitt, D. P. Abraham,
D. D. Keiser, Jr.,** and J. Y. Park***
Chemical Technology Division
Argonne National Laboratory
9700 South Cass Avenue
Argonne, Illinois 60439

RECEIVED
JUL 18 1996
OSTI

The submitted manuscript has been authored by a contractor of the U.S. Government under contract No. W-31-109-ENG-38. Accordingly, the U.S. Government retains a nonexclusive, royalty-free license to publish or reproduce the published form of this contribution, or allow others to do so, for U.S. Government purposes.

To be Presented at:
SPECTRUM International Conference on
Nuclear and Hazardous Waste Management
Seattle, Washington
August 18-23, 1996

*Work supported by the U.S. Department of Energy, Nuclear Energy Research & Development Program, Contract W-31-109-Eng-38.

**Engineering Division (ED).

***Energy Technology Division.

DISCLAIMER

**Portions of this document may be illegible
in electronic image products. Images are
produced from the best available original
document.**

STAINLESS STEEL-ZIRCONIUM ALLOY WASTE FORMS

S. M. McDeavitt, D. P. Abraham, D. D. Keiser, and J. Y. Park
Chemical Technology Division/Energy Technology Division
Argonne National Laboratory
9700 South Cass Avenue
Argonne, IL 60439, USA

INTRODUCTION

An electrometallurgical treatment process has been developed by Argonne National Laboratory to convert various types of spent nuclear fuels into stable storage forms and waste forms for repository disposal [1,2]. The first application of this process will be to treat spent fuel alloys from the Experimental Breeder Reactor-II (EBR-II), located in the Idaho National Engineering Laboratory (near Idaho Falls, Idaho, USA). Electrometallurgical treatment refers to the set of operations required to break down spent fuel and convert the various constituents into stable forms. This process involves electrorefining uranium and other actinides from chopped fuel pins in a molten salt electrolyte. Three distinct product streams emanate from the electrorefining process [1-4]: (1) refined uranium; (2) fission products and actinides extracted from the electrolyte salt that are processed into a mineral waste form; and (3) metallic wastes left behind at the completion of the electrorefining step. The third product stream (i.e., the metal waste stream) is the subject of this paper.

The metal waste stream contains components of the chopped spent fuel that are unaffected by the electrorefining process because of their electrochemically "noble" nature [3]; this includes the cladding hulls, noble metal fission products (NMFP), and, in specific cases, zirconium from metal fuel alloys. The cladding hulls comprise the majority (>80 wt%) of the metal waste stream and, therefore, dominate the composition of the waste form alloy. The noble metal fission products include radioactive isotopes of Ru, Rh, Pd, Tc, Mo, Zr, Ag, and many other metal elements in increasingly minor quantities; the elements listed represent the most prevalent noble metal fission products in the waste stream [3].

The NMFP content in the waste stream depends on fuel burnup, but it does not exceed 5 wt% of the final waste form at high burnup. Zirconium metal is a prevalent fuel component (e.g., EBR-II driver fuel contains 10 wt% Zr) and, therefore, represents a significant waste form component for certain fuel types.

The selected method for the consolidation and stabilization of the metal waste stream is melting and casting into a uniform, corrosion-resistant alloy. The waste form casting process will be carried out in a controlled-atmosphere furnace at high temperatures with a molten salt flux. Spent fuels with both stainless steel and Zircaloy cladding are being evaluated for treatment; thus, stainless steel-rich and Zircaloy-rich waste forms are being developed. The nominal waste form compositions that have been selected for full development are stainless steel-15 wt% zirconium (SS-15Zr) and Zircaloy-8 wt% stainless steel (Zr-8SS), with each containing 1 to 5 wt% NMFP.

Stainless steel-zirconium alloys containing actinide metals are also of interest for two reasons: (1) the cladding hulls will contain an actinide residue left over after electrorefining, and (2) the ultimate disposition of the transuranic (TRU) -bearing product stream is being evaluated, and its incorporation in the metal waste form is under consideration. Although the primary disposition option for the actinides is the mineral waste form, the concept of incorporating the TRU-bearing product into the metal waste form has enough potential to warrant investigation.

NON-TRU WASTE FORM ALLOYS

Small-scale samples of stainless steel-zirconium (SS-Zr) alloys were generated with a range of zirconium compositions to simulate the SS-15Zr and Zr-8SS waste forms and off-normal alloy compositions. The alloy samples were prepared from stainless steel (Type HT9, 304, or 316), zirconium, and noble metal additions such as Ru, Pd, Mo, and Ag. Alloy samples of ~20 g were contained in

yttria (Y_2O_3) crucibles and melted at 1600°C in an argon atmosphere for 1 to 2 h and solidified by cooling slowly. The argon cover gas contained less than 10 ppm oxygen and water. The alloy samples produced were of uniform microstructure and low porosity. In the yttria (Y_2O_3) crucibles containing steel-rich melts (i.e., <25 wt% Zr), crucible-melt interactions were not observed. In contrast, Zr-rich melts (i.e., >50 wt% Zr) resulted in minor dissolution of the Y_2O_3 . The samples were sectioned, polished, and examined using a scanning electron microscope (SEM). In addition, energy dispersive X-ray analysis (EDX), was used for quantitative composition analysis of individual phases

Stainless steel-rich SS-Zr alloys contained varying proportions of ferritic and austenitic phases of stainless steel along with a brittle Laves intermetallic $Zr(Fe,Cr,Ni)_{2+x}$. The proportion of $Zr(Fe,Cr,Ni)_{2+x}$ in the alloy microstructure increased with increasing zirconium concentration until ~40 wt% Zr, when the alloy is ~100% intermetallic. The Fe-Zr phase diagram indicates that a eutectic occurs at 15.1 wt% Zr, and the nominal waste form composition, SS-15Zr (Fig. 1), possessed a eutectic microstructure.

The zirconium-rich SS-Zr alloys contained multi-phase mixtures of a zirconium solid solution and various intermetallic phases up to ~84 wt% Zr (16 wt% SS). Compositions between 40 and 84 wt% Zr resulted in multiple intermetallic phases with no metal phases present; completely intermetallic waste forms would be very brittle and unacceptable. Between 84 and 100 wt% Zr, the SS-Zr alloys contained increasing proportions of an α -Zr solid solution phase. The nominal waste form composition, Zr-8SS (Fig. 2), possessed a multi-phase microstructure dominated by the primary α -Zr solid solution surrounded by a complex eutectic structure containing the α -Zr solution and intermetallics, which were qualitatively identified as $Zr_2(Fe,Ni)$ and $Zr(Fe,Cr)_2$.

The noble metals Ru, Pd, Mo, and Ag were added to the SS-15Zr and Zr-8SS waste form samples using the above methods for non-radioactive samples. In

addition, rhenium and technetium (Tc-99) were added by the methods used to generate the TRU-bearing specimens described in the next section. Noble metal additions did not result in the formation of discrete phases that would be indicative of fission product segregation. For the SS-15Zr alloy, all of the noble metals were dissolved and distributed into both the intermetallic and the iron solution phases. Some metals (i.e., Ru, Pd, and Ag) showed a preference for the intermetallic phase, while others (i.e., Rh) showed a preference for the iron solution phases. The noble metal distribution has not yet been quantified for the Zr-8SS alloy.

TRU-BEARING WASTE FORM ALLOYS

Nine small-scale samples of simulated waste form alloys (~30 g) containing U, Pu, and Np were placed in yttria crucibles and cast in an induction furnace. Two castings were made per furnace run. The melting procedure involved heating the furnace to 1600°C for 2 h with a flowing argon atmosphere, then cooling slowly to room temperature. The test samples include six SS-15Zr alloys with cast compositions (in wt%) of (0.5U-0.5Pu), (2U-2Pu), 6Pu, 10Pu, (6Pu-2Np), and 2Np and three Zr-8SS alloys with 4, 7, and 10 wt% Pu. The SS-15Zr alloys were generated using Type 316SS, and the Zr-8SS alloys were generated using Type 304SS. The samples were sectioned, polished, and examined using SEM and EDX methods.

Figure 3 presents a representative microstructure for the TRU-bearing SS-15Zr alloys. The microstructure is similar to the two-phase SS-15Zr eutectic structure (Fig. 1) except for the presence of a third phase that is rich in actinides. The dark iron solution phase and $Zr(Fe,Cr,Ni)_2$ intermetallic are nearly identical to the corresponding phases in the non-TRU samples. There is 2 atom % Pu in the intermetallic but no actinides in the iron solution phase. The high-contrast phases in Fig. 3 are rich in actinides. (in the SS-15Zr-10Pu sample, these phases contained 20 atom % Pu.) This third phase is apparently an intermetallic that is

miscible with the $Zr(Fe,Cr,Ni)_2$ intermetallic, and its composition is essentially 33 atom % Fe-33 atom % Ni-20 atom % actinide (U, Pu, and/or Np) plus small amounts of Zr, Cr, and minor components. This phase was observed in all of the TRU-bearing SS-15Zr alloys, irrespective of the actinide or group of actinides present; increasing the actinide content resulted in a higher volume fraction of this phase.

Figure 4 presents a representative microstructure for the Zr-8SS-xPu alloys. Again, the microstructure resembles the non-TRU alloy (Fig. 2). In contrast to the SS-15Zr alloys, the added plutonium was found to be in the metal α -Zr solution phase, not in the intermetallics. Plutonium was observed in solution in the α -Zr matrix, but it also was found in higher concentrations at the α -phase boundaries. The β -Zr phase has a significantly higher solubility for plutonium than α -Zr; the high-temperature β -Zr and ϵ -Pu phases are completely miscible. The zirconium metal precipitates as β -Zr with up to 100% of the plutonium in solution, but as it transforms to α -Zr at $\sim 863^\circ\text{C}$, the plutonium becomes concentrated at the newly formed boundaries. For the alloy compositions that were examined, increasing the amount of plutonium added to the alloy resulted in higher amounts of plutonium both in the α -Zr matrix phase and at the α -phase boundaries.

WASTE FORM PROCESSING AND EVALUATION

In parallel with the laboratory-scale characterization of the above alloys, processing methods are being developed for full-scale production of metal waste forms. The first application of the electrometallurgical treatment will be to process EBR-II spent fuel in the Fuel Conditioning Facility (FCF) at Argonne National Laboratory - West. Because the fuel cladding from EBR-II consists of Types 304, 316, and D9 stainless steels [5], the SS-15Zr waste form alloy will be

generated. The alloy D9 is similar to Type 316 stainless steel, with a small amount of titanium (0.2-0.3 wt %) and a higher Ni/Cr ratio.

To develop the required processing methodology for waste form production in the FCF, a tilt-pour induction casting furnace that is connected to an inert atmosphere glovebox was designed and built. In this furnace, large-scale ingots of SS-15Zr alloy (~3 kg) have been generated by melting at 1600°C with and without a molten CaCl₂ salt flux. The salt flux is a processing option that may be useful for radionuclide containment and the generation of clean alloys. The molten waste form alloy is a very reactive liquid metal, primarily because it contains zirconium. Therefore, the process requires a high-purity, inert atmosphere and a stable material for containing the melt. Yttria crucibles have been used in the small-scale experiments (~1.7-cm dia) and in the tilt-pour furnace (10-cm dia), but yttria has very poor thermal shock resistance, which limits the furnace heating rate to less than ~10°C/min. Alternative containment materials and processing techniques (e.g., cold-crucible methods) are being sought to overcome this limitation.

Both large- and small-scale alloy ingots were used to generate specimens for testing and evaluation. Small-scale samples with various zirconium contents were machined and polished into disks (~1.6-cm dia) and tested using general and electrochemical corrosion methods in simulated J-13 well water. The J-13 well water is representative of the groundwater at the Yucca Mountain site in Nevada that has been proposed for a high-level nuclear waste repository. The estimated electrochemical corrosion rate (solution at pH=7) for both SS-15Zr and Zr-8SS alloys is approximately 0.02 to 0.03 MPY* (4 to 6 g/m²/yr), which is comparable or less than the measured rates for Types 316 and 304 stainless steel (0.04 to 0.05 MPY) and zirconium metal (0.06 to 0.10 MPY). Large-scale ingots with 15 wt% Zr from the tilt-pour furnace were machined into additional corrosion test specimens and also into mechanical test specimens. Uniaxial tension tests on the SS-15Zr alloy have resulted in almost no elongation and

* Mils per year.

reduction in area, but the alloy is quite strong with a fracture strength that is as high or greater than the yield strength for hardened stainless steel.

REFERENCES

- [1] J. E. Battles, J. J. Laidler, C. C. McPheeters, and W. E. Miller, "Pyrometallurgical Processes for Recovery of Actinide Elements," in Actinide Processing: Methods and Materials, eds. B. Mishra and W. A. Averill (The Minerals, Metals & Materials Society, Warrendale, PA, 1994) 135.
- [2] J. P. Ackerman, "Chemical Basis for Pyrochemical Reprocessing of Nuclear Fuel," Ind. Eng. Chem. Res., 30 (1991) 141.
- [3] S. M. McDeavitt, J. Y. Park and J. P. Ackerman, "Defining a Metal Waste Form for IFR Pyroprocessing Wastes," in Actinide Processing: Methods and Materials, eds. B. Mishra and W. A. Averill (The Minerals, Metals & Materials Society, Warrendale, PA, 1994) 305.
- [4] J. P. Ackerman, T. R. Johnson, and J. J. Laidler, "Waste Removal in Pyrochemical Fuel Processing for the Integral Fast Reactor," in Actinide Processing: Methods and Materials, eds. B. Mishra and W. A. Averill (The Minerals, Metals & Materials Society, Warrendale, PA, 1994) 261.
- [5] L. C. Walters, B. R. Seidel, and J. H. Kittel, "Metallic Fuels and Blankets in LMFBRs," Nuclear Technology, 65 (1984) 202.

DISCLAIMER

This report was prepared as an account of work sponsored by an agency of the United States Government. Neither the United States Government nor any agency thereof, nor any of their employees, makes any warranty, express or implied, or assumes any legal liability or responsibility for the accuracy, completeness, or usefulness of any information, apparatus, product, or process disclosed, or represents that its use would not infringe privately owned rights. Reference herein to any specific commercial product, process, or service by trade name, trademark, manufacturer, or otherwise does not necessarily constitute or imply its endorsement, recommendation, or favoring by the United States Government or any agency thereof. The views and opinions of authors expressed herein do not necessarily state or reflect those of the United States Government or any agency thereof.

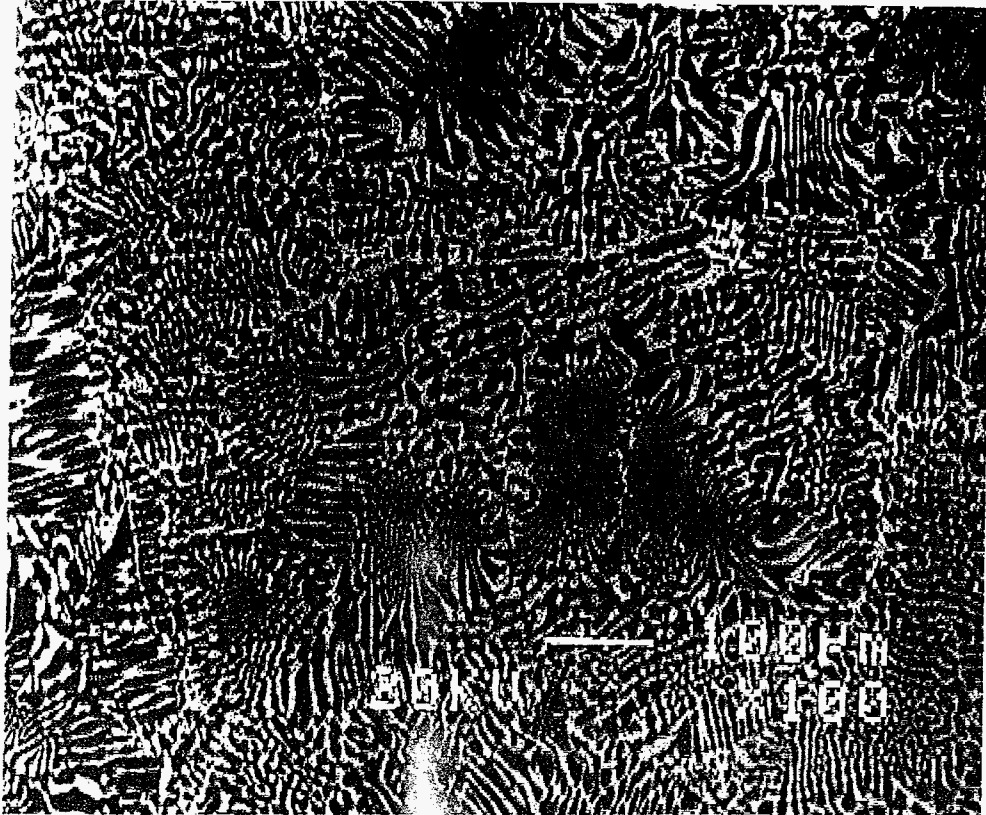


Fig. 1. Backscattered Electron Image (500x) of the SS-15Zr Eutectic Structure. The dark phase is an iron solid solution, and the bright phase is the $Zr(Fe,Cr,Ni)_{2+x}$ intermetallic.

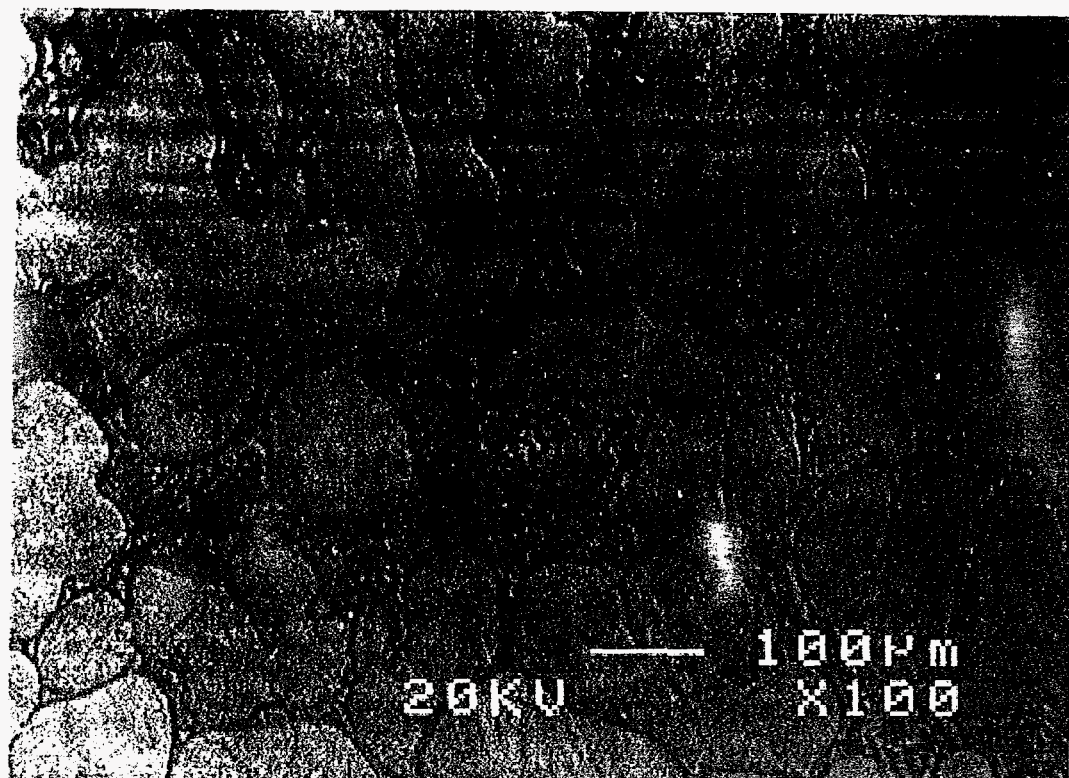


Fig. 2. Backscattered Electron Image (100x) of the Zr-8SS Structure. The gray major phase is a zirconium solid solution, and the darker phases are intermetallics.

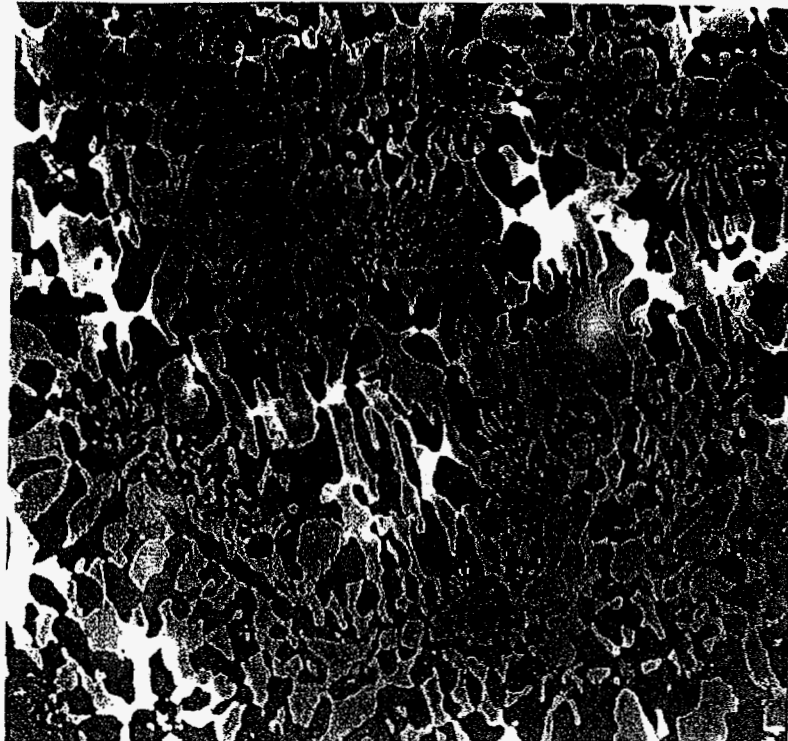


Fig. 3. Backscattered Electron Image of SS-15Zr Alloy Containing 2 wt% U and 2 wt% Pu. The bright contrast phases are rich in U and Pu.



Fig. 4. Backscattered Electron Image of Zr-8SS Alloy Containing 10 wt% Pu. The Zr solution phase contains some plutonium, but the bright-contrast features indicate high plutonium contents at α -phase boundaries.